



HAL
open science

Supraventricular cardiac conduction system exposure in breast cancer patients treated with radiotherapy and association with heart and cardiac chambers doses

M.Y. Errahmani, Medea Locquet, David Broggio, D. Spoor, G. Jimenez, J. Camilleri, J.A. Langendijk, A.P.G. Crijs, Marie-Odile Bernier, J. Ferrières, et al.

► To cite this version:

M.Y. Errahmani, Medea Locquet, David Broggio, D. Spoor, G. Jimenez, et al.. Supraventricular cardiac conduction system exposure in breast cancer patients treated with radiotherapy and association with heart and cardiac chambers doses. *Clinical and Translational Radiation Oncology*, 2023, 38, pp.62-70. 10.1016/j.ctro.2022.10.015 . hal-04020918

HAL Id: hal-04020918

<https://hal.science/hal-04020918v1>

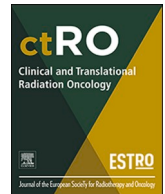
Submitted on 9 Mar 2023

HAL is a multi-disciplinary open access archive for the deposit and dissemination of scientific research documents, whether they are published or not. The documents may come from teaching and research institutions in France or abroad, or from public or private research centers.

L'archive ouverte pluridisciplinaire **HAL**, est destinée au dépôt et à la diffusion de documents scientifiques de niveau recherche, publiés ou non, émanant des établissements d'enseignement et de recherche français ou étrangers, des laboratoires publics ou privés.



Distributed under a Creative Commons Attribution 4.0 International License



Supraventricular cardiac conduction system exposure in breast cancer patients treated with radiotherapy and association with heart and cardiac chambers doses

M.Y. Errahmani^{a,b}, M. Locquet^a, D. Broggio^c, D. Spoor^d, G. Jimenez^e, J. Camilleri^e, J.A. Langendijk^d, A.P.G. Crijs^d, M.O. Bernier^a, J. Ferrières^f, J. Thariat^g, S. Boveda^h, Y. Kirovaⁱ, P. Loapⁱ, V. Monceau^j, S. Jacob^{a,*}

^a Laboratory of Epidemiology, Institute for Radiation Protection and Nuclear Safety (IRSN), Fontenay-Aux-Roses, France

^b University Paris-Saclay, Gif-sur-Yvette, France

^c Department of Dosimetry, IRSN/PSE-SANTE/SDOS/LEDI, Institute for Radiation Protection and Nuclear Safety (IRSN), Fontenay-Aux-Roses, France

^d Department of Radiation Oncology, University Medical Center Groningen (UMCG), University of Groningen, Groningen, the Netherlands

^e Department of Radiation Oncology (Oncorad), Clinique Pasteur, Toulouse, France

^f Department of Cardiology and INSERM UMR 1295 CERPOP, Rangueil University Hospital, Toulouse, France

^g Department of Radiotherapy, Centre de Lutte Contre le Cancer A. Baclesse, University of Caen Normandie, Caen, France

^h Heart Rhythm Management Department, Clinique Pasteur, Toulouse, France

ⁱ Department of Radiation Oncology, Institut Curie, Paris, France

^j Laboratory of Radiotoxicology and Radiobiology, Institute for Radiation Protection and Nuclear Safety (IRSN), Fontenay-Aux-Roses, France

ARTICLE INFO

Keywords:

Breast cancer
Radiation therapy
Conduction nodes
Arrhythmias
Conduction disorders
Dosimetry

ABSTRACT

Purpose: To assess sinoatrial node (SAN) and atrioventricular node (AVN) doses for breast cancer (BC) patients treated with 3D-CRT and evaluate whether “large” cardiac structures (whole heart and four cardiac chambers) would be relevant surrogates.

Material and methods: This single center study was based on 116 BCE patients (56 left-sided, 60 right-sided) treated with 3D-CRT without respiratory gating strategies and few IMN irradiations from 2009 to 2013. The heart, the left and right ventricles (LV, RV), the left and right atria (LA, RA) were contoured using multi-atlases for auto-segmentation. The SAN and the AVN were manually delineated using a specific atlas. Based on regression analysis, the coefficients of determination (R^2) were estimated to evaluate whether “large” cardiac structures were relevant surrogates ($R^2 > 0.70$) of SAN and AVN doses.

Results: For left-sided BC, mean doses were: 3.60 ± 2.28 Gy for heart, 0.47 ± 0.24 Gy for SAN and 0.74 ± 0.29 Gy for AVN. For right-sided BC, mean heart dose was 0.60 ± 0.25 Gy, mean SAN dose was 1.57 ± 0.63 Gy (>85 % of patients with SAN doses > 1 Gy) and mean AVN dose was 0.51 ± 0.14 Gy. Among all “large” cardiac structures, RA appeared as the best surrogate for SAN doses ($R^2 > 0.80$). Regarding AVN doses, the RA may also be an interesting surrogate for left-sided BC ($R^2 = 0.78$), but none of “large” cardiac structures appeared as relevant surrogates among right-sided BC (all $R^2 < 0.70$), except the LA for patients with IMN ($R^2 = 0.83$).

Conclusions: In BC patients treated 10 years ago with 3D-CRT, SAN and AVN exposure was moderate but could exceed 1 Gy to the SAN in many right-sided patients with no IMN-inclusion. The RA appeared as an interesting surrogate for SAN exposure. Specific conduction nodes delineation remains necessary by using modern radiotherapy techniques.

Introduction

Adjuvant radiotherapy (RT) is commonly used as a treatment

modality for localized breast cancer (BC), resulting in improved tumour control and reduced cancer-related death risk [1–2]. However, BC survivors can develop a wide spectrum of radiation-associated cardiac

* Corresponding author at: IRSN, PSE-SANTE, SESANE, LEPID, BP17, 92262 Fontenay-aux-Roses cedex, France.

E-mail address: sophie.jacob@irsn.fr (S. Jacob).

<https://doi.org/10.1016/j.ctro.2022.10.015>

Received 21 September 2022; Received in revised form 27 October 2022; Accepted 30 October 2022

Available online 4 November 2022

2405-6308/© 2022 The Authors. Published by Elsevier B.V. on behalf of European Society for Radiotherapy and Oncology. This is an open access article under the CC BY-NC-ND license (<http://creativecommons.org/licenses/by-nc-nd/4.0/>).

diseases, arising from few months to many years after RT [3–5]. Cardiac arrhythmias and conduction disorders have been previously described as radiation-induced complications of BC irradiation [6]. The conduction system can be directly injured by radiation through an inflammatory process resulting in fibrosis of the conduction pathways or nodal structures (sino atrial and atrioventricular nodes) or via fibrosis after ischemia of the myocardium due to microvascular damage. The tissue fibrosis induced by RT could be responsible for non-specific secondary cardiac lesions at the atrial, ventricular, and coronary levels, which are the basis for arrhythmia and bradycardia. But these arrhythmias and conduction disorders could also potentially be due to direct damage to critical cardiac structures, such as the sino-atrial node and the atrioventricular node. Several cases reports suggested that radiation was associated prolonged QT interval, ventricular tachycardia, sinus node dysfunction, atrioventricular blocks, and bundle branch blocks [7–10], but also in several cohort studies. Patients receiving RT for BC had a higher risk of cardiac arrhythmia and conduction disorders morbidity and mortality compared to those without RT [11–12]. These results were confirmed in a recent study indicating that BC patients who underwent RT had a 2.2-fold increased risk of conduction disorders requiring pacemaker implantation, compared to the general population [13]. Another large cohort of >14,000 cancer patients recently concluded that RT for cancer was an independent risk factor for atrial fibrillation [14].

Dose-response relationships between cardiac exposure and the risk to develop arrhythmia and conduction disorders have been poorly studied in BC patients, in contrast with coronary diseases for which associations with the mean heart dose were observed [15–16]. Regarding the risk of cardiac arrhythmia and conduction disorders, a recent case-control study performed in a population of BC patients treated with RT, suggested that right-sided BC patients may require particular attention, and the dose to the right atrium may be a more relevant dosimetric parameter than the mean heart dose or other cardiac chambers dose metrics [17]. Many types of conduction disorders can happen anywhere along the cardiac conduction system: at the sino-atrial node (SAN), the atrioventricular node (AVN), or the bundle branches. The SAN is located in the wall of the right atrium. The AVN is also located in the right atrium, close to the interatrial septum and the coronary sinus ostium. In the previously described case-control study [17], the authors suggested that the association found between higher risk for right-sided BC and RA dose may be related to the location of the SAN and conductive tissue in the right atrium and prompted to further investigate specifically these conduction nodes dosimetry.

The dose received by the cardiac conduction nodes during BC irradiation has never been evaluated at the scale of an epidemiologic study. Recently, a RT contouring atlas for SAN and AVN delineation was published [18], providing the opportunity to evaluate the dose received by these nodes for BC patients treated with RT. However, manually delineating of SAN and AVN can be time-consuming and cardiac auto-segmentation algorithms for such small structures still remains to be validated at large scale [19]. Therefore, it is also of interest to evaluate whether larger cardiac structures (heart, left and right ventricles, left and right atria), with available multi-atlas-based auto-segmentation algorithm (MABAS) [20], could be used as surrogates for conduction node exposure.

The aim of this dosimetric study was to evaluate the radiation exposure of cardiac conduction nodes (SAN and AVN) in BC patients treated with three-dimensional conformal radiation therapy (3D-CRT) from 2009 to 2013 and to evaluate whether larger cardiac structures (the whole heart and the four cardiac chambers) would be relevant surrogates to assess these nodes dosimetry in historical cohorts.

Material and methods:

Study population

Our dosimetric study was based on a previously described population of BC patients treated with adjuvant radiotherapy (3D-CRT) for either right or left-sided BC at Clinique Pasteur in Toulouse between January 2009 and December 2013 [17].

After the surgical treatment of BC, all patients were treated with 3D-CRT with or without regional lymph node irradiation. For most patients, 6 MV photons beams by tangential fields were used, except few cases of patients with large breasts where 25 MV photons were used. The prescribed dose to the planning target volume dose was mostly 50 Gy delivered in 25 daily fractions of 2 Gy over 5 weeks. In rare cases of elderly patients who received RT to the breast without lymph node irradiation, the total dose of 32.5 Gy was delivered in 5 weekly fractions of 6.5 Gy. Additional boost of 9–15 Gy could be applied to the tumour site using photon/electron beams with energies ranging from 6 MeV to 18 MeV. The treatment planning system (TPS) used to perform dose calculations was Eclipse™ with the Analytical Anisotropic Algorithm (AAA v13.6) (Varian Medical System, Palo Alto, CA, USA). Each patient's RT was planned such that the dose distribution was optimized and normalized to the International Commission on Radiation Units and Measurements (ICRU) reference point of the breast and to achieve QUANTEC dose constraints to organs at risk including the heart [21], and deep-inspirational breath-hold (DIBH) technique was used for very few left-sided patients.

Cardiac structures delineation and dosimetry

For all patients, large cardiac structures delineation was performed by UMCG using MABAS. The whole heart (WH) and the four cardiac chambers, including the left and right ventricles (LV, RV), and the left and right atria (LA, RA) were delineated using the in house MABAS tool based on the atlas by Feng et al [22] (Mirada RTx [version 1.6]; Mirada Medical, Oxford, United Kingdom) Spoor et al., 2021.

The SAN and AVN were subsequently manually delineated on the CT planning scans according to previously published guidelines [18]. The SAN was delineated as a 2 cm-diameter sphere, tangent to the external wall of the right atrium, centred at the height of the ascending aorta origin and the AVN was delineated as a 2 cm-diameter sphere centered at the junction between the four cardiac chambers, 1 cm above the last slice where the left atrium was visible.

Using the 3D dose matrix generated during treatment planning and the new delineated substructures, dose-volume histograms for the whole heart and the four cardiac chambers (LV, RV, LA and LV) from the UMCG side, and for the SAN and AVN from the IRSN side, were generated with RayStation and ISOgray TPS respectively (Fig. 1).

Statistical analysis

For all delineated cardiac structures (WH, LV, LA, RV, RA, SAN, AVN), the mean doses (Dmean) and near-maximum doses (D2) were retrieved from the dose-volume histograms. Descriptive analysis of the physical doses in Gray (Gy) was performed. Continuous variables are presented as mean, standard deviation and range values. Categorical values are presented as percentages. To compare categorical variables, we used chi-square tests, whereas for continuous variables we used the non-parametric Wilcoxon tests. Pearson correlation coefficients were calculated between dose to the SAN and AVN and dose to the whole heart and the four cardiac chambers. The relationship analysis between mean dose to large cardiac structures and mean doses to the SAN and AVN were further investigated based on linear regressions providing the R² value which corresponded to the coefficient of determination indicating the proportion of the variance in Dmean of SAN and AVN predictable from Dmean of WH, LV, LA, RV and RA. The arbitrary value of

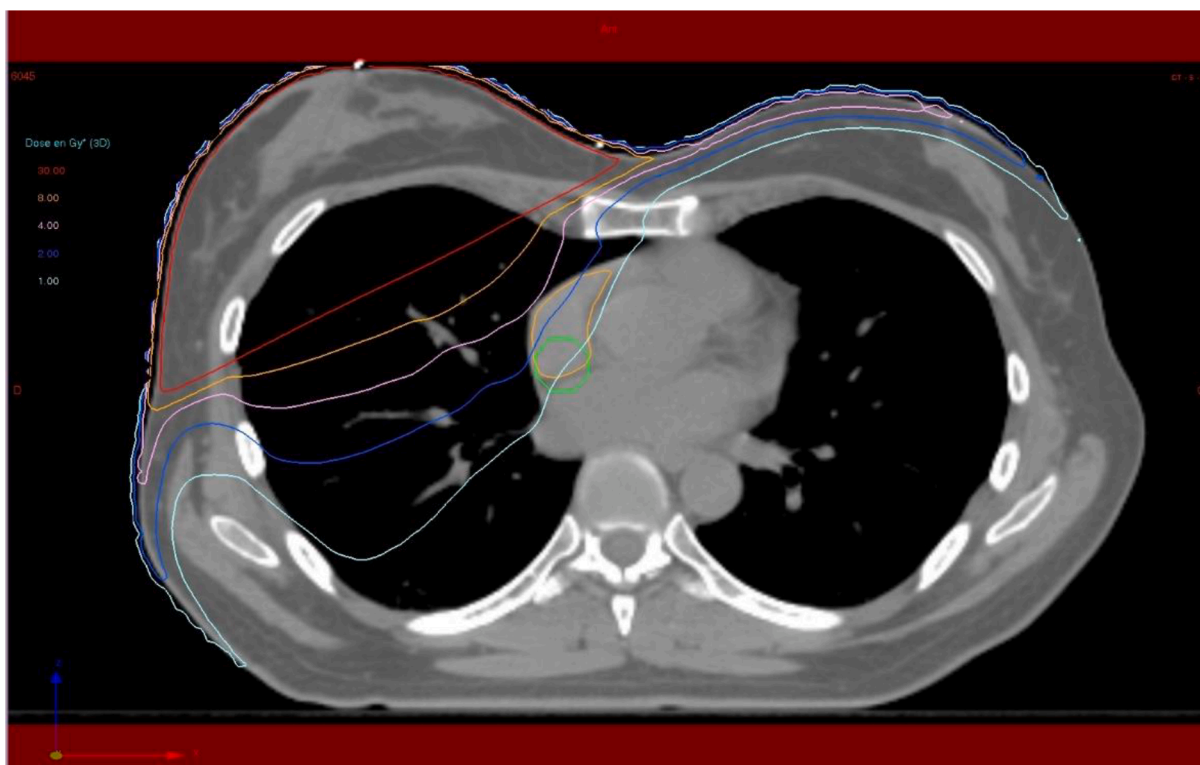


Fig. 1. CT dose-planned right tangential breast irradiation showing isodoses and delineated structures: right atrium (RA) in orange and sinoatrial node (SAN) in green. (For interpretation of the references to colour in this figure legend, the reader is referred to the web version of this article.)

$R^2 > 0.70$ was considered good for prediction with a surrogate delineated structure. $P < 0.05$ was considered statistically significant. Statistical analyses were performed with SAS version 9.4 (SAS Institute Inc, Cary, NC).

Results:

Patient characteristics

Patient, tumour and treatment characteristics are presented in Table 1. The study was based on 116 BCE patients (56 left-sided and 60 right-sided). Mean age at RT was 64 ± 10 years, without any significant difference between left- and right-sided BC patients ($p = 0.90$). About 65 % of patients were diagnosed with invasive ductal carcinoma and almost all (91 %) underwent breast-conserving surgery. The prescribed dose was 50 Gy in 25 sessions for 92 % of the population and almost three-fourths had an additional boost delivered to the tumour site. Regional lymph node irradiation was performed in 33 % of patients, which were equally distributed in both BC-sided groups ($p = 0.87$). Only 18 patients had IMN-inclusion.

Description of doses according to BC laterality

Dosimetric parameters for the whole heart, the four cardiac chambers, the SAN and the AVN are presented in Table 2. The mean heart dose was 3.60 ± 2.28 Gy for left-sided RT and 0.60 ± 0.25 Gy for right-sided RT. As for the mean heart dose, we observed higher mean doses to the LV the RV and the LA for left-sided BC compared to right-sided BC (4.81 ± 2.95 Gy vs 0.16 ± 0.08 Gy for LV; 3.65 ± 3.57 Gy vs 0.64 vs 0.27 Gy for RV; 0.87 ± 0.63 Gy vs 0.43 ± 0.16 Gy for LA, all $p < 0.0001$). However, for the RA, doses were higher for right-sided BC compared to left-sided BC (1.45 ± 0.63 vs 0.51 ± 0.26 Gy, $p < 0.001$). Among right-sided BC, 88 % of patients received a mean RA dose above 1 Gy (7 % among left-sided BC). In addition, near-maximum doses D2 for

Table 1
Patients characteristics.

	All patients (n = 116)	Left-sided BC (n = 56)	Right-sided BC (n = 60)	p-value
Age at BC diagnosis, in years	64.4 ± 10.34	64.3 ± 10.3	64.6 ± 10.6	0.90
Histology, N (%)				
Invasive ductal carcinoma	75 (65 %)	33 (60 %)	42 (70 %)	0.72
Invasive lobular carcinoma	11 (10 %)	6 (11 %)	5 (8 %)	
Invasive tubular carcinoma	7 (6 %)	4 (7 %)	3 (5 %)	
Mixed or other carcinoma	23 (20 %)	13 (23 %)	10 (17 %)	
Type of surgery, N (%)				
Lumpectomy	105 (91 %)	49 (88 %)	56 (93 %)	0.52
Mastectomy	10 (9 %)	6 (11 %)	4 (7 %)	
Prescription dose, N (%)				
32.5 Gy (5 × 6.5 Gy)	7 (6 %)	4 (7 %)	3 (5 %)	0.92
40.05 Gy (15 × 2.67 Gy)	1 (1 %)	0 (0 %)	1 (2 %)	
47 Gy (20 × 2.35 Gy)	1 (1 %)	0 (0 %)	1 (2 %)	
50 Gy (25 × 2 Gy)	107 (92 %)	52 (93 %)	55 (92 %)	
Additional boost, N (%)	88 (76 %)	43 (77 %)	45 (75 %)	0.83
Regional lymph node irradiation, N (%)	38 (33 %)	19 (34 %)	19(32)	0.87
Supraclavicular	20 (17 %)	7 (13)	13 (22 %)	
IMN	4 (3 %)	0 (0 %)	4 (7 %)	
Both	14 (12 %)	12 (21 %)	2 (3 %)	
Adjuvant chemotherapy, N (%)	37 (32 %)	16 (29 %)	21 (35 %)	0.55
Adjuvant endocrine therapy, N (%)	82 (71 %)	40 (71 %)	42 (70 %)	1.00

BC: Breast cancer; IMN: Internal Mammary Node.

RA was 3.76 Gy on average (range: 0.75 – 15.56 Gy). Regarding conduction nodes, impact of laterality for SAN exposure was similar to that observed for RA, with higher SAN doses for right-sided BC versus left-sided BC (1.57 ± 0.63 Gy vs 0.47 ± 0.24 Gy, $p < 0.0001$). >85 % of right-sided BC received mean SAN dose >1 Gy (4 % for left-sided BC),

Table 2
Dosimetric parameters for the heart, cardiac chambers, and conduction nodes.

	Left-sided BC N = 56		Right-sided BC N = 60		p-value
	Mean ± SD	Range	Mean ± SD	Range	
Heart					
Dmean (Gy)	3.60 ± 2.28	0.80–11.44	0.60 ± 0.25	0.03–1.43	<0.0001
D2 (Gy)	30.33 ± 17.02	3.54–50.34	2.99 ± 1.94	0.34–11.77	<0.0001
Left Ventricle					
Dmean (Gy)	4.81 ± 2.95	1.01–13.23	0.16 ± 0.08	0.00–0.45	<0.0001
D2 (Gy)	29.69 ± 17.16	2.64–50.64	0.58 ± 0.34	0.00–2.73	<0.0001
Right Ventricle					
Dmean (Gy)	3.65 ± 3.57	0.69–18.97	0.64 ± 0.27	0.00–1.59	<0.0001
D2 (Gy)	19.51 ± 17	2.12–47.47	1.98 ± 1.39	0.00–9.39	<0.0001
Left Atrium					
Dmean (Gy)	0.87 ± 0.63	0.22–3.70	0.43 ± 0.16	0.00–0.94	<0.0001
D2 (Gy)	2.47 ± 2.90	0.60–16.57	0.93 ± 0.39	0.01–2.50	0.0003
Right Atrium					
Dmean (Gy)	0.51 ± 0.26	0.13–1.27	1.45 ± 0.63	0.59–4.12	<0.0001
D2 (Gy)	1.03 ± 0.85	0.21–5.24	3.76 ± 2.54	0.75–15.56	<0.0001
Sinoatrial Node					
Dmean (Gy)	0.47 ± 0.24	0.09–1.28	1.57 ± 0.63	0.59–4.04	<0.0001
D2 (Gy)	0.59 ± 0.32	0.12–2.09	2.41 ± 1.24	0.83–8.13	<0.0001
Atrioventricular node					
Dmean (Gy)	0.74 ± 0.29	0.24–1.48	0.51 ± 0.14	0.26–0.91	<0.0001
D2 (Gy)	0.92 ± 0.41	0.29–2.58	0.64 ± 0.19	0.31–1.30	0.0002

BC breast cancer, SD: standard deviation, D2 minimal dose received by the most irradiated 2% of the structure volume, Dmean: mean dose to the structure.

and near-maximum dose ranged from 0.83 Gy to 8.13 Gy. For the AVN, impact of laterality on exposure was similar to that observed for WH, LV RV and LA, with higher doses for left-sided BC compared to right-sided BC (0.74 ± 0.29 Gy vs 0.51 ± 0.14 Gy, p < 0.0001). No patient received AVN dose > 1 Gy in right-sided BC, and 18 % in left-sided BC. Separate analysis for patients with or without IMN are presented in Table 3. Irradiation of IMN resulted in higher doses to all structures with a factor ranging from 1.7 to 2.9 for heart, LV and RV among left sided patients (<1.4 for other structures), whereas for right-sided patients, the highest factor was observed for RA and SAN (1.8 and 1.6 respectively).

Association between SAN and AVN doses and doses to the whole heart and the four cardiac chambers

The ratios of Dmean SAN and Dmean AVN over Dmean heart and Dmean cardiac chambers are presented in Table 4, as well as the correlations between Dmean nodes and Dmean larger structures Regarding SAN, the ratios were all < 1 for left-sided BC (indicating lower dose to SAN than to other structures) and > 1 for right-sided BC (indicating higher doses to SAN than to other structures). However, the ratio was close to one with RA dose for both lateralities (0.94 for left-sided, 1.07 for right-sided). The highest correlations were observed with the mean RA dose (r = 0.94 for left-sided and 0.92 for right-sided BC). With a ratio of 2.6, the correlation with mean heart dose was also high for right-sided

Table 3
Mean doses to the heart, cardiac chambers and conduction nodes according to irradiation status of Internal Mammary Nodes.

	Left-sided BC		Right-sided BC	
	IMN included N = 12	Without IMN N = 44	IMN included N = 6	Without IMN N = 54
Heart				
Dmean (Gy)	5.72 ± 2.27	3.02 ± 1.94	0.89 ± 0.29	0.57 ± 0.22
Left Ventricle				
Dmean (Gy)	7.20 ± 2.8	4.15 ± 2.66	0.20 ± 0.06	0.17 ± 0.11
Right Ventricle				
Dmean (Gy)	7.56 ± 5.03	2.58 ± 2.10	0.84 ± 0.37	0.62 ± 0.25
Left Atrium				
Dmean (Gy)	1.11 ± 0.66	0.80 ± 0.61	0.53 ± 0.15	0.44 ± 0.24
Right Atrium				
Dmean (Gy)	0.66 ± 0.19	0.47 ± 0.26	2.38 ± 1.06	1.35 ± 0.48
Sinoatrial Node				
Dmean (Gy)	0.62 ± 0.16	0.50 ± 0.50	2.39 ± 0.95	1.50 ± 0.53
Atrioventricular node				
Dmean (Gy)	0.93 ± 0.28	0.68 ± 0.27	0.56 ± 0.14	0.53 ± 0.23

Table 4
Association parameters between mean doses to the SAN and AVN and the mean doses to the heart and cardiac chambers.

	Sinoatrial Node		Atrioventricular Node	
	Left-sided BC	Right-sided BC	Left-sided BC	Right-sided BC
Heart				
Ratio Dmean Node/ Dmean Heart (median)	0.14	2.58	0.21	0.88
Correlation Dmean Node & Dmean Heart (r, p-value)	0.72, p < 0.001	0.85, p < 0.001	0.85, p < 0.001	0.68, p < 0.001
Left Ventricle				
Ratio Dmean Node/ Dmean LV (median)	0.10	9.31	0.16	3.14
Correlation Dmean Node & Dmean LV (r, p-value)	0.57, p < 0.001	0.56, p < 0.001	0.75, p < 0.001	0.74, p < 0.001
Right Ventricle				
Ratio Dmean Node/ Dmean RV (median)	0.17	2.45	0.30	0.82
Correlation Dmean Node & Dmean RV (r, p-value)	0.64, p < 0.001	0.69, p < 0.001	0.73, p < 0.001	0.65, p < 0.001
Left Atrium				
Ratio Dmean Node/ Dmean LA (median)	0.59	3.43	0.97	1.16
Correlation Dmean Node & Dmean LA (r, p-value)	0.74, p < 0.001	0.69, p < 0.001	0.76, p < 0.001	0.83, p < 0.001
Right Atrium				
Ratio Dmean Node/ Dmean RA (median)	0.94	1.07	1.53	0.37
Correlation Dmean Node & Dmean RA (r, p-value)	0.96, p < 0.001	0.92, p < 0.001	0.88, p < 0.001	0.51, p < 0.001

BC Breast Cancer, LV left ventricle, RV Right Ventricle, LA left Atrium, RA Right Atrium.

BC (r = 0.85). Regarding the AVN, ratios > 1 were observed for RA among left-sided BC (1.53) and for LV and LA for right-sided BC (3.14 and 1.16 respectively). In terms of correlation, the highest coefficients were observed with mean heart dose for left-sided BC (r = 0.85) and with LA dose for right-sided BC (r = 0.83).

Linear regression between Dmean for SAN and AVN and Dmean for heart and cardiac chambers are presented in Figs. 2 and 3. As indicated

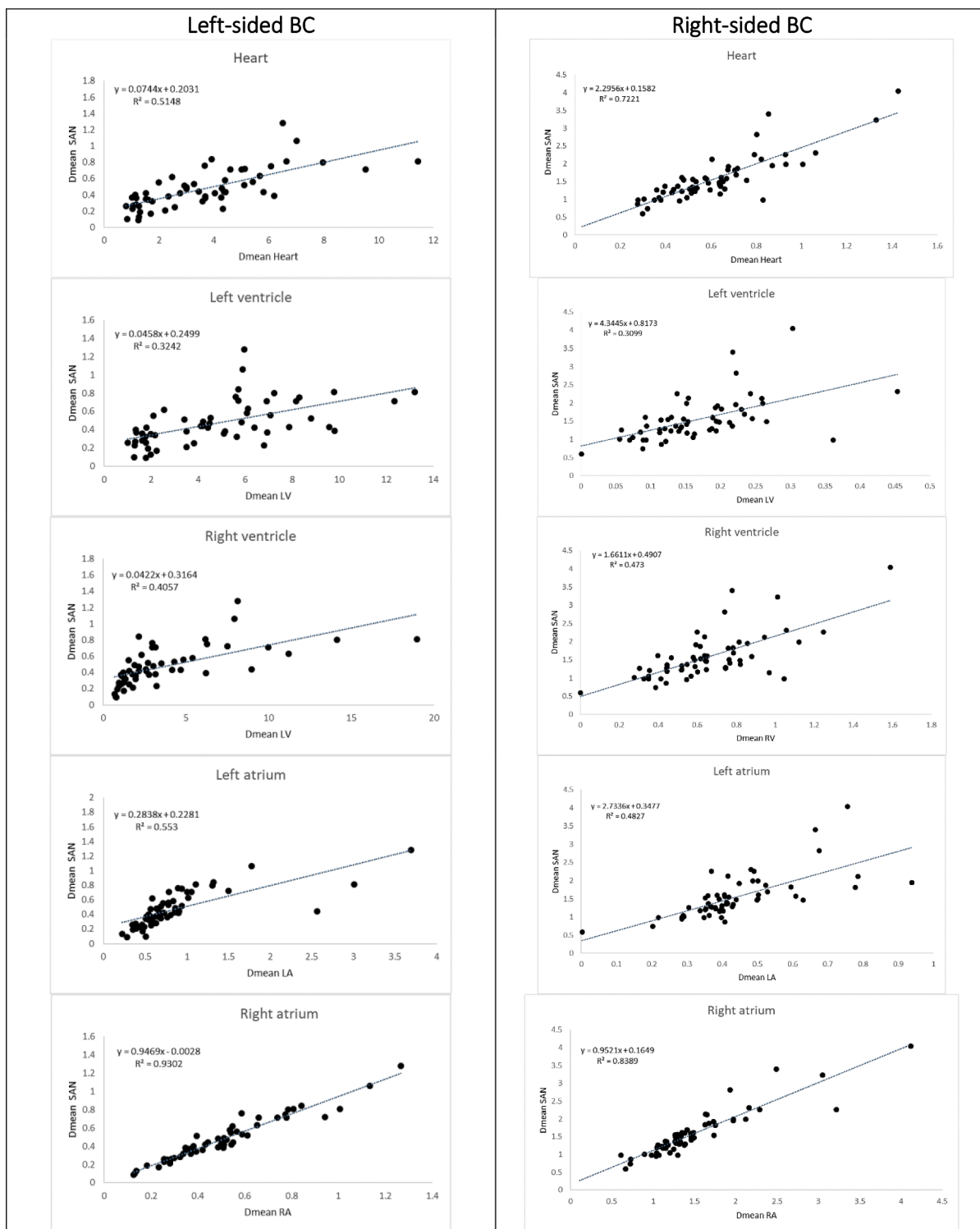


Fig. 2. Relationship between Dmean SAN and mean doses to the heart and cardiac chambers.

previously, a cut-off value of 0.7 for R^2 was considered for potentially accurate prediction of nodes doses using a surrogate structure. For the SAN dose, the RA dose was very good to excellent in both lateralities ($R^2 = 0.93$ and 0.84) and mean heart dose was good for right-sided BC ($R^2 = 0.72$). However, for right-sided BC patients with a mean heart dose ≥ 0.60 Gy (50 % of right-sided BC), the R^2 decreased to 0.60, whereas for right-sided BC patients with mean heart dose < 0.60 Gy, the R^2 was 0.83. For right-sided BC patients with mean RA dose > 1.35 Gy (50 % of right-sided BC) the R^2 decreased but remained good with a value of 0.75 but

the R^2 was decreased to 0.64 when considering patients with RA dose < 1.35 Gy. For AVN dose, a $R^2 > 0.70$ could be observed only for mean heart dose ($R^2 = 0.72$) and mean RA dose ($R^2 = 0.78$) among left-sided BC. However, among right-sided BC, with no R^2 value above 0.70, none of “large” cardiac structures could be considered good enough for AVN dose prediction. Only the LA dose reached a R^2 value close to 0.70 ($R^2 = 0.68$).

Separate analysis for patients with IMN are presented in Table 5. We could observe similar results as those presented for the whole cohort for

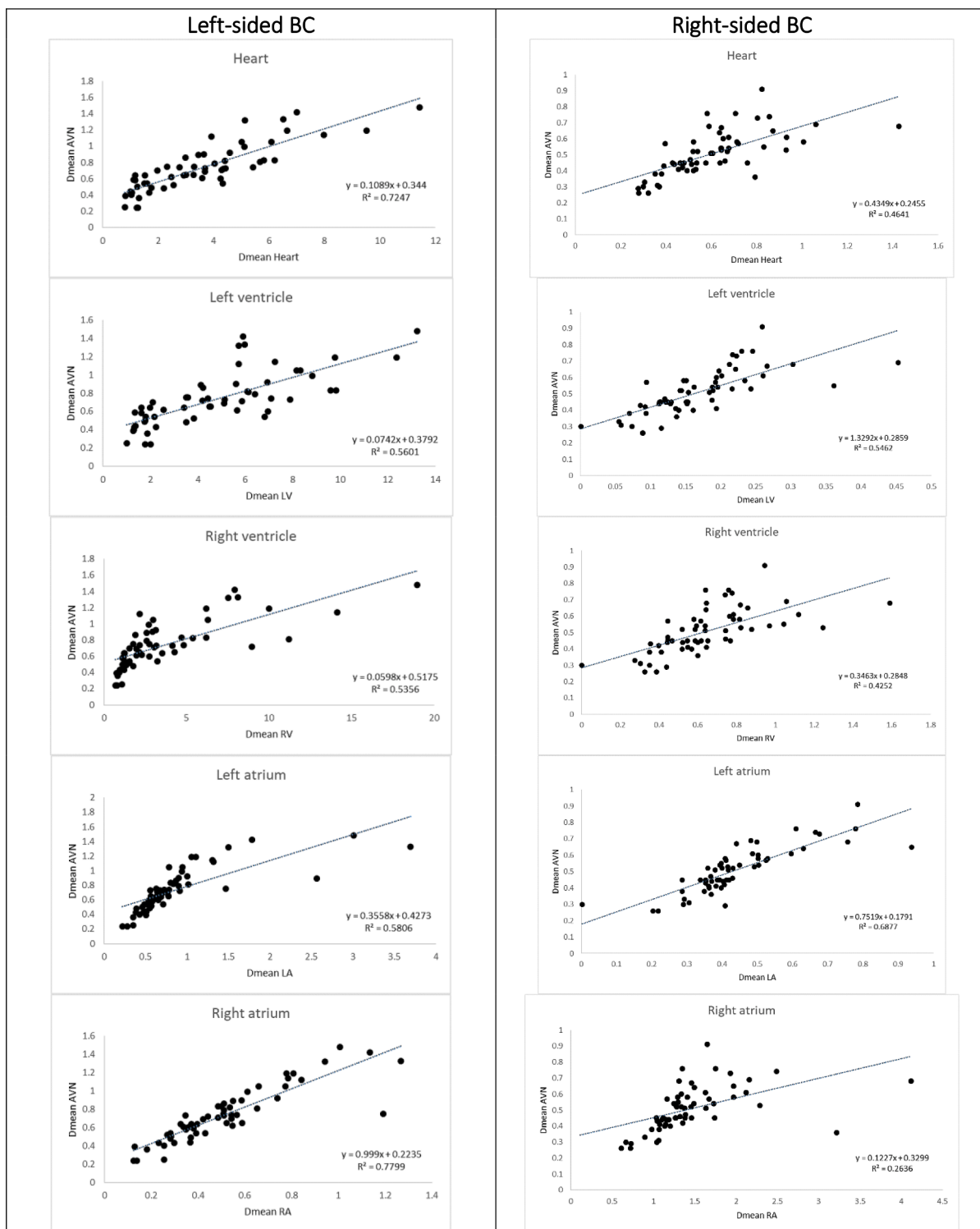


Fig. 3. Relationship between Dmean AVN and mean doses to the heart and cardiac chambers.

SAN: the RA dose reached R² values > 0.70 (0.79 in left-sided patients, 0.71 in right-sided patients). For AVN, RA and LA appeared as a good predictor for left-sided patients with R² = 0.88 and 0.74 respectively, but for right-sided patients LA reached R² value of 0.83 which was not so strong for the whole cohort (R² = 0.68).

Discussion:

This dosimetric study has three main findings regarding conduction

nodes exposure in the context of BC irradiation performed 10 years ago with 3D-CRT without respiratory gating strategies and few IMN irradiation. First, we observed that mean doses to the SAN and AVN remained in a moderate range of exposure for left and right-sided BC (<1.6 Gy). Second, the SAN and the RA were the most exposed cardiac substructures for right-sided BC with >85 % of patients receiving doses >1 Gy (reaching >4 Gy for some patients), in contrast with whole heart, LV, RV, LA and AVN where doses remained < 1 Gy for >90 % of right-sided BC patients. Third, the RA dose was a good candidate as surrogate of

Table 5

For BC patients with IMN: association parameters between mean doses to the SAN and AVN and the mean doses to the heart and cardiac chambers.

	Sinoatrial Node		Atrioventricular Node	
	Left-sided BC with IMN	Right-sided BC with IMN	Left-sided BC with IMN	Right-sided BC with IMN
Heart				
Ratio Dmean Node/ Dmean Heart (median)	0.11	2.83	0.17	0.64
Correlation Dmean Node × Dmean Heart (r, p-value)	0.54, <i>p</i> = 0.07	0.86, <i>p</i> = 0.03	0.79, <i>p</i> = 0.002	0.50, <i>p</i> = 0.31
R ²	0.29	0.72	0.62	0.25
Left Ventricle				
Ratio Dmean Node/ Dmean LV (median)	0.09	12.92	0.13	2.69
Correlation Dmean Node × Dmean LV (r, p-value)	0.31, <i>p</i> = 0.33	0.79, <i>p</i> = 0.06	0.65, <i>p</i> = 0.023	0.71, <i>p</i> = 0.11
R ²	0.09	0.62	0.42	0.50
Right Ventricle				
Ratio Dmean Node/ Dmean RV (median)	0.10	2.89	0.16	0.66
Correlation Dmean Node × Dmean RV (r, p-value, r2)	0.5, <i>p</i> = 0.11	0.82, <i>p</i> = 0.046	0.68, <i>p</i> = 0.014	0.53, <i>p</i> = 0.284
R ²	0.25	0.67	0.46	0.28
Left Atrium				
Ratio Dmean Node/ Dmean LA (median)	0.63	4.22	0.93	1.08
Correlation Dmean Node × Dmean LA (r, p-value)	0.62, <i>p</i> = 0.031	0.83, <i>p</i> = 0.04	0.86, <i>p</i> = 0.0003	0.91, <i>p</i> = 0.011
R ²	0.38	0.69	0.74	0.83
Right Atrium				
Ratio Dmean Node/ Dmean RA (median)	0.98	1.00	1.44	0.30
Correlation Dmean Node × Dmean RA (r, p-value)	0.89, <i>p</i> = 0.001	0.84, <i>p</i> = 0.03	0.94, <i>p</i> < 0.001	0.1, <i>p</i> = 0.84
R ²	0.79	0.71	0.88	0.01

IMN: internal mammary node; R²: proportion of the variance in Dmean Node that can be explained by the Dmean large structure in the regression model (R² > 0.70 in bold corresponding to strong association).

SAN doses in both lateralities and good potential of AVN dose in left laterality only. However, for right-sided BC, none of “large” cardiac structure could be considered as a good surrogate parameter of AVN dose, except for patients with IMN where LA may be interesting.

This is the first study providing a detailed dose description of conduction nodes in the context of BC irradiation with 3D-CRT. We observed that right-sided RT exposed the SAN with an average mean dose of 1.6 Gy, more than twice the observed mean heart dose values (around 0.6 Gy). Such ratio was previously observed for mediastinal irradiation for Hodgkin Lymphoma [23] but the distribution of heart exposure was different from our population. However, right-sided RT did not induce high doses to the AVN (mean = 0.51 Gy, range 0.26 – 0.91 Gy). This could be explained by the location of these nodes: the SAN is located on the right side of the right atrium which is the most exposed area for right-sided irradiation, whereas the AVN is more central, at the junction between the four cardiac chambers which results in less pronounced difference in exposure according to laterality (mean dose = 0.14 Gy for left-sided BC and 0.51 Gy for right-sided BC).

Previous studies have suggested an excess risk of arrhythmia and conduction disorders after RT for BC [13,17]. Conduction disorders may occur anywhere along the cardiac conduction system, at the SAN, the AVN or the bundle branches. Cardiac exposure is characterized by important heterogeneity among cardiac substructures [24] and mean heart dose which is the most commonly used dosimetric parameter presents limitations for comprehension of radiation-induced

cardiotoxicity. Recent studies have demonstrated that dosimetric parameters of specific cardiac substructures were associated with clinical or subclinical events: dose to the LAD associated with acute coronary event [25,26], dose to the LV associated with subclinical LV dysfunction [27,28] in particular. This still need to be proven for arrhythmia and conduction disorders, but a recent case-control study suggested that RA dose may be more relevant than mean heart dose [17], such association possibly related to the location of the SAN, and conductive tissue in the RA.

Further investigation on conduction nodes dosimetry is thus justified. But manual delineation of SAN and AVN can be time-consuming and cardiac auto-segmentation algorithms for such small structure remains to be validated at large scale [19]. Therefore, it was also of interest to evaluate whether larger cardiac structures (heart, left and right ventricles, left and right atria), with available multi-atlas-based auto-segmentation algorithm (MABAS) [20], could be used as surrogates for conduction nodes exposure in retrospective cohorts investigating dose–response relationship for cardiac arrhythmia and conduction disorders.

Person correlation coefficients between dose to the heart and to the SAN and AVN were previously evaluated for mediastinal Hodgkin lymphoma irradiation with volumetric modulated arc therapy [23]. The mean SAN dose was 6.6 Gy and the mean AVN dose was 0.9 Gy. Correlation coefficients with mean heart dose were 0.72 for SAN and 0.87 for AVN. Despite higher doses than ours to the SAN (0.47 Gy and 1.57 Gy for left and right-sided BC in our study) and to the AVN (0.74 Gy and 0.51 Gy for left and right-sided BC in our study), these results are consistent with our results on BC population: for SAN, our r coefficients were 0.72 and 0.85 for left and right-sided BC respectively; for AVN, our r coefficients were 0.85 and 0.68 for left and right-sided BC respectively. Both studies indicated that dosimetric parameters of the heart, of the SAN and of the AVN were imperfectly correlated. We observed that the R² coefficient with mean heart dose was high for SAN in left-sided BC but low in right-sided BC (R² = 0.72 and 0.46) and was high for AVN in right-sided BC but low for left-sided BC (R² = 0.72 and 0.51). In addition, for right-sided patients with higher mean heart doses the R² decreased to lower value (R² = 0.60). Consequently, despite that the mean heart dose is the most widely used dosimetric parameter, for cardiotoxicity purpose, regarding conduction disorder, this dosimetric parameter showed limitations as surrogate of conduction nodes exposure.

To our knowledge, no study previously assessed the relevance of cardiac chambers doses as surrogates of conduction nodes doses. We observed that the RA had the best potential to predict SAN dose with R² values of 0.93 and 0.84 for left and right-sided BC. However, for right-sided BC with the highest RA dose (>0.6 Gy), the R² value was decreased to 0.60 indicating that RA is far to be a perfect surrogate of SAN dose. For AVN dose, despite a good R² value for RA dose in left-sided BC, no cardiac structure appeared as good surrogate (R² values < 0.60) which may again be explained by the central position of the AVN, making this small structure more difficult to assess by larger cardiac structure. As a consequence, our study illustrates that precise evaluation of dose to SAN and AVN requires specific delineation and reinforces the interest to further develop automatic segmentation of these nodes [19].

Despite a moderate range of doses for SAN and AVN in BC patients treated with 3D-CRT, we observed that for right-sided BC, the SAN was the most exposed cardiac structure which may explain previous results suggesting a higher risk of arrhythmia and conduction disorders for right-sided BC compared to left sided-BC and a potential association with the RA dose [17]. However, it remained to be explored whether the SAN and AVN doses are associated with that risk, which would provide arguments in favour of a causality association between conduction system exposure and conduction disorders which is still only hypothesized. If such association is confirmed, in the future, development of normal tissue complication probability (NTCP) models based on

dosimetric parameters to the SAN and to the AVN, could finally allow proposing dose constraints for these conduction structures. Conduction disorders are often lifelong and require continuous care. Complications of conduction disorders may be serious or life-threatening. It is thus important to enhance knowledge on this specific category of radiation-induced cardiovascular diseases in patients treated with radiotherapy in order to further develop prevention.

Limitations

We acknowledge that this study has some limitations. First, the cohort comes from a single center for BC patients treated 10 years ago, and therefore might be influenced by their local planning practice. This might limit the generalizability of the doses reported and correlations observed and prompts to further develop research on that topic based on current practices. All our BC patients were treated with 3D-CRT, in few cases IMN irradiation was performed, and we did not consider modern techniques of RT (IMRT, VMAT, Proton therapy and other adapted techniques). Moreover, no impact of DIBH could be assessed on conduction system exposure as only 4 left-sided patients experienced DIBH. Most of our patients (92 %) were treated with 50 Gy +/- boost, with 2 Gy per fraction. However, volume of irradiation could be breast alone or breast and lymph nodes, some treatments were hypofractionated (7 patients) and we did not specifically analyse these subgroups of patients because of the limited sample size. Nevertheless, our patients were all treated with the same technique, and this is the first study providing results on conduction nodes doses in more than a hundred of BC patients treated with RT. Moreover, analysis performed on the subgroup of 107 patients (92 % of the sample) all treated with 50 Gy with 2 Gy per fraction provided similar results to those presented here (data not shown). Doses were extracted from two different TPS (RayStation for heart and cardiac chambers, ISOgray for conduction nodes). This may have a slight impact on doses as each TPS has a slightly different way of calculating DVH parameters. However, this was not a major concern here, since the TPS was consistent for each substructure across the cohort. Delineation of SAN and AVN is quite recent. We used previously published atlas methodology and our manually-delineated contours were validated by the Institut Curie team who developed the atlas. However, such delineation can be difficult, based on 2-cm sphere around the potential localization of the nodes which indeed are not visible structure on the CT scans. We focused our analysis on supraventricular cardiac conduction system including the SAN and the AVN which are identifiable on CT-scans and reproducibly delineated [18,29]. The SAN and AVN exposure assessment may be more relevant for supraventricular arrhythmias and conduction disorders but not for ventricular arrhythmias. Causal association between SAN / AVN exposure and risk of arrhythmias and conduction disorders remains to be investigated.

Conclusions

In BC patients treated 10 years ago with 3D-CRT, SAN and AVN exposure was moderate but could exceed 1 Gy to the SAN in many right-sided patients and even reach several Gray. RA appeared as an interesting surrogate for SAN exposure, but no cardiac structure stood out as a good predictor of AVN dose, except LA for patient with IMN. In future studies, conduction nodes delineation will be necessary to precisely evaluate the potential association with the risk of supraventricular arrhythmias and conduction disorders.

Declaration of Competing Interest

The authors declare that they have no known competing financial interests or personal relationships that could have appeared to influence the work reported in this paper.

Data Availability Statement

The datasets used and/or analyzed during the current study are available from the corresponding author on reasonable request.

Ethical consideration.

The study was subject to a declaration of compliance with a reference methodology concerning research in the field of health (MR 03) from the French Commission Informatique et Liberté - CNIL, (ref 2103119, September 27, 2017). For collection of data in medical records, all patients were provided information letter and non-objection notice concerning the study.

Funding

H2020 Euratom research and training program 2014–2018 under grant agreement No 755523 in the frame of the MEDIRAD project.

Acknowledgements

We thank Ludovic De Marzi, medical physicist in Institut Curie (Paris) who participated in the images treatment before delineation validation of SAN and AVN. This work was supported by H2020 Euratom research and training program 2014–2018 under grant agreement No 755523 in the frame of the MEDIRAD project.

References

- [1] Darby S, McGale P, Correa C, et al. Effect of radiotherapy after breast-conserving surgery on 10-year recurrence and 15-year breast cancer death: meta-analysis of individual patient data for 10,801 women in 17 randomised trials. *Lancet* 2011; 378:1707–16.
- [2] Taylor C, Correa C, Duane FK, Aznar MC, Anderson SJ, Bergh J, et al. Estimating the Risks of Breast Cancer Radiotherapy: Evidence From Modern Radiation Doses to the Lungs and Heart and From Previous Randomized Trials. *J Clinical Oncol* 2017;35(15):1641–9.
- [3] Clarke M, Collins R, Darby S, et al. Effects of radiotherapy and of differences in the extent of surgery for early breast cancer on local recurrence and 15-year survival: an overview of the randomised trials. *Lancet* 2005;366:2087–106.
- [4] McGale P, Darby SC, Hall P, Adolfsen J, Bengtsson N-O, Bennet AM, et al. Incidence of heart disease in 35,000 women treated with radiotherapy for breast cancer in Denmark and Sweden. *Radiation Oncology* 2011;100(2):167–75.
- [5] Bergom C, Bradley JA, Ng AK, Samson P, Robinson C, Lopez-Mattei J, et al. Past, Present, and Future of Radiation-Induced Cardiotoxicity: Refinements in Targeting, Surveillance, and Risk Stratification. *JACC CardioOncology* 2021;3(3):343–59.
- [6] Heidenreich PA, Kapoor JR. Radiation induced heart disease: systemic disorders in heart disease. *Heart* 2009;95:252–8.
- [7] Messina F, Romano P, Paino M, Crosca S. Long-term complication of the thoracic radiation in breast cancer: An complete atrioventricular block case. *Int J Cardiol* 2016;202:5–6.
- [8] Orzan F, Brusca A, Gaita F, Giustetto C, Figliomeni MC, Libero L. Associated cardiac lesions in patients with radiation-induced complete heart block. *Int J Cardiol* 1993;39(2):151–6.
- [9] Slama MS, Guludec D, Sebag C, et al. Complete atrioventricular block following mediastinal irradiation: a report of six cases. *PACE* 1991;14(7):1112–8.
- [10] Larsen RL, Jakacki RI, Vetter VL, Meadows AT, Silber JH, Barber G. Electrocardiographic changes and arrhythmias after cancer therapy in children and young adults. *Am. J. Cardiology* 1992;70(1):73–7.
- [11] Leung HWC, Chan ALF, Muo C-H. Late cardiac morbidity of adjuvant radiotherapy for early breast cancer - A population-based study. *J Cardiol* 2016;67(6):567–71.
- [12] Wu SP, Tam M, Vega RM, Perez CA, Gerber NK. Effect of Breast Irradiation on Cardiac Disease in Women Enrolled in BCIRG-001 at 10-Year Follow-Up. *Int J Radiat Oncol Biol Phys* 2017;99(3):541–8.
- [13] Errahmani MY, Thariat J, Ferrières J, Panh L, Locquet M, Lapeyre-Mestre M, et al. Risk of pacemaker implantation after radiotherapy for breast cancer: A study based on French nationwide health care database sample. *International journal of cardiology Heart & vasculature* 2022;38:100936.
- [14] Apte N, Dherange P, Mustafa U, Ya'qoub L, Dawson D, Higginbotham K, et al. Cancer Radiation Therapy May Be Associated With Atrial Fibrillation. *Frontiers in cardiovascular medicine* 2021;8:610915.
- [15] Darby SC, Ewertz M, McGale P, Bennet AM, Blom-Goldman U, Brønnum D, et al. Risk of ischemic heart disease in women after radiotherapy for breast cancer. *The New England journal of medicine* 2013;368(11):987–98.
- [16] van den Bogaard VAB, Ta BDP, van der Schaaf A, Bouma AB, Middag AMH, Bantema-Joppe EJ, et al. Validation and Modification of a Prediction Model for Acute Cardiac Events in Patients With Breast Cancer Treated With Radiotherapy Based on Three-Dimensional Dose Distributions to Cardiac Substructures. *Journal of clinical oncology : official journal of the American Society of Clinical Oncology* 2017;35(11):1171–8.
- [17] Errahmani MY, Locquet M, Spoor D, Jimenez G, Camilleri J, Bernier M-O, et al. Association between cardiac radiation exposure and the risk of arrhythmia in

- breast cancer patients treated with radiotherapy: a case-control study. *Front Oncol* 2022;12:892882.
- [18] Loap P, Servois V, Dhonneur G, Kirov K, Fourquet A, Kirova Y. A radiotherapy contouring atlas for cardiac conduction node delineation. *Practical radiation oncology* 2021.
- [19] Loap P, De Marzi L, Kirov K, Servois V, Fourquet A, Khoubeyb A, et al. Development of Simplified Auto-Segmentable Functional Cardiac Atlas. *Practical radiation oncology* 2022;12(6):533–8.
- [20] Spoor DS, Sijtsma NM, van den Bogaard VAB, van der Schaaf A, Brouwer CL, Ta BDP, et al. Validation of separate multi-atlases for auto segmentation of cardiac substructures in CT-scans acquired in deep inspiration breath hold and free breathing. *Radiotherapy and oncology : journal of the European Society for Therapeutic Radiology and Oncology* 2021;163:46–54.
- [21] Gagliardi G, Constine LS, Moiseenko V, Correa C, Pierce LJ, Allen AM, et al. Radiation dose-volume effects in the heart. *Int J Radiat Oncol Biol Phys* 2010;76(3):S77–85.
- [22] Feng M, Moran JM, Koelling T, Chughtai A, Chan JL, Freedman L, et al. Development and validation of a heart atlas to study cardiac exposure to radiation following treatment for breast cancer. *Int J Radiat Oncol Biol Phys* 2011;79(1): 10–8.
- [23] Loap P, Mirandola A, De Marzi L, Vitolo V, Barcellini A, Iannalfi A, et al. Cardiac conduction system exposure with modern radiotherapy techniques for mediastinal Hodgkin lymphoma irradiation. *Acta Oncol* 2022;61(4):496–9.
- [24] Jacob S, Camilleri J, Derreumaux S, Walker V, Lairez O, Lapeyre M, et al. Is mean heart dose a relevant surrogate parameter of left ventricle and coronary arteries exposure during breast cancer radiotherapy: a dosimetric evaluation based on individually-determined radiation dose (BACCARAT study). *Radiat Oncol* 2019;14(1).
- [25] Atkins KM, Chaunzwa TL, Lamba N, Bitterman DS, Rawal B, Bredfeldt J, et al. Association of Left Anterior Descending Coronary Artery Radiation Dose With Major Adverse Cardiac Events and Mortality in Patients With Non-Small Cell Lung Cancer. *JAMA oncology* 2021;7(2):206.
- [26] van den Bogaard VAB, Spoor DS, van der Schaaf A, van Dijk LV, Schuit E, Sijtsma NM, et al. The Importance of Radiation Dose to the Atherosclerotic Plaque in the Left Anterior Descending Coronary Artery for Radiation-Induced Cardiac Toxicity of Breast Cancer Patients? *Int J Radiat Oncol Biol Phys* 2021;110(5): 1350–9.
- [27] Walker V, Lairez O, Fondard O, Pathak A, Pinel B, Chevelle C, et al. Early detection of subclinical left ventricular dysfunction after breast cancer radiation therapy using speckle-tracking echocardiography: association between cardiac exposure and longitudinal strain reduction (BACCARAT study). *Radiat Oncol* 2019;14(1).
- [28] Locquet M, Spoor D, Crijns A, van der Harst P, Eraso A, Guedea F, et al. Subclinical Left Ventricular Dysfunction Detected by Speckle-Tracking Echocardiography in Breast Cancer Patients Treated With Radiation Therapy: A Six-Month Follow-Up Analysis (MEDIRAD EARLY-HEART study). *Front Oncol* 2022;12:883679.
- [29] Loap P, Tkatchenko N, Nicolas E, Fourquet A, Kirova Y. Optimization and auto-segmentation of a high risk cardiac zone for heart sparing in breast cancer radiotherapy. *Radiotherapy and oncology : journal of the European Society for Therapeutic Radiology and Oncology* 2020;153:146–54.